



Estimation of soybean softening based on Raman spectral analysis of solubilized components in cooking water

Wenchao Li^a, Takashi Watanabe^b, Kasumi Nakagawa^c, Takahisa Nishizu^{c,d},
Tepei Imaizumi^{c,d,*} 

^a United Graduate School of Agricultural Science, Gifu University, 1-1 Yanagido, Gifu City, Gifu, 501-1193, Japan

^b Institute of Food Research, NARO, 2-1-12, Kannondai, Tsukuba, Ibaraki, 305-8642, Japan

^c Faculty of Applied Biological Sciences, Gifu University, 1-1 Yanagido, Gifu, 501-1193, Japan

^d Preemptive Food Research Center, Gifu University, 1-1 Yanagido, Gifu City, Gifu, 501-1193, Japan

ARTICLE INFO

Keywords:

Raman spectroscopy
Soybean
Protein denaturation
Pectin solubilization
Thermal softening

ABSTRACT

Dynamic and nondestructive monitoring of soybean softening during thermal processing is essential for ensuring consistent texture and quality in processed foods. However, achieving accurate and nondestructive assessment remains challenging, particularly in sealed high-temperature cooking conditions. Therefore, this study investigated the molecular changes in the proteins and pectin released into water during soybean boiling and their relationship with textural softening. Raman spectroscopy, both with and without the use of ethanol as an internal standard, was utilized to capture spectral variations. This was supported by chemical quantification of protein and pectin concentrations and texture analysis. Principal component analysis identified key Raman peaks at 682 cm^{-1} (C-S), 558 cm^{-1} (S-S), and 936 cm^{-1} (glycosidic linkages), reflecting the accumulation of solubilized components and correlating strongly with textural softening ($R^2 = 0.69\text{--}0.73$). The addition of ethanol improved spectral stability across replicates without interfering with key molecular signals, enabling more consistent detection. These findings demonstrate that Raman spectroscopy, when standardized with an internal reference, offers a reliable, nondestructive method to assess soybean softening in real time. This approach provides a foundation for future applications in legume quality monitoring and industrial thermal processing control.

1. Introduction

Soybeans (*Glycine max*) are a globally important legume crop valued for their high protein content (40–42 % by dry weight) and essential nutrients (Rahman et al., 2011). In addition to their traditional applications in products such as natto and tofu, soybeans have gained increasing attention in ready-to-eat products due to rising demand for convenient and nutritious foods (Pedone et al., 2024). To improve flavor and nutrient bioavailability, thermal processing methods like boiling are commonly employed (Sasipriya & Siddhuraju, 2012). In industrial settings, high-pressure cooking systems have been adopted to shorten cooking duration and ensure uniform softening. However, these closed systems hinder temporal monitoring of texture development, often leading to inconsistent product quality.

In food processing, achieving optimal softening is critical for ensuring product palatability, reducing energy costs, and meeting industrial standards for texture consistency. Texture, particularly

hardness, is a key indicator of quality in processed soybeans and influences consumer acceptance. Softening during thermal treatment is primarily directed by biochemical changes such as starch gelatinization, protein denaturation, and pectin solubilization (Chigwedere et al., 2018; Kyomugasho et al., 2023). Among these, protein denaturation and pectin solubilization are the critical factors contributing to tissue breakdown. Thermal treatment causes the unfolding of proteins, thereby exposing hydrophobic regions and sulfhydryl groups, which may result in aggregation and reduced functionality (Aryee et al., 2018; Kong et al., 2023). Meanwhile, pectin is a primary component of the middle lamella and undergoes solubilization upon heating, weakens intercellular adhesion, and promotes cell separation (Chigwedere et al., 2018; L. Zhang & McCarthy, 2013; Zhu, Che, et al., 2023). The extent of polygalacturonic acid release is closely associated with texture loss (Van Buren, 1979). Although starch granules swell during cooking, their effects on structural changes are considered secondary (Chen et al., 2022).

As these key components leach into the cooking water, their analysis

* Corresponding author. Faculty of Applied Biological Sciences, Gifu University, 1-1 Yanagido, Gifu, 501-1193, Japan.

E-mail address: imaizumi.tepei.j6@f.gifu-u.ac.jp (T. Imaizumi).

<https://doi.org/10.1016/j.lwt.2025.118535>

Received 3 June 2025; Received in revised form 30 August 2025; Accepted 21 September 2025

Available online 22 September 2025

0023-6438/© 2025 The Authors. Published by Elsevier Ltd. This is an open access article under the CC BY license (<http://creativecommons.org/licenses/by/4.0/>).

offers a promising, non-destructive strategy for assessing structural degradation. Various spectroscopic techniques, including near-infrared (NIR), Fourier transform infrared (FTIR), and ultraviolet–visible (UV–Vis) spectroscopy, have been applied to monitor soluble components in aqueous matrices. For instance, NIR spectroscopy has successfully predicted the dry matter content in soaking water (Lukacs et al., 2025), and FTIR has been applied to quantify soluble pectin in orange juice, especially when enhanced by chemometric models (Bizzani et al., 2020). Despite their demonstrated potential, these methods often require extensive calibration, advanced statistical modeling, and high-performance instrumentation, which can limit their applicability for temporal monitoring. Furthermore, all these techniques face internal limitations in aqueous environments. NIR and FTIR suffer from strong water absorption bands that interfere with weak molecular signals from target solutes (Chang et al., 2018; Liu et al., 2022), whereas UV–Vis is generally limited to chromophoric compounds and is not suitable for the direct detection of colorless molecules, such as proteins and pectin.

Given the limitations of these techniques, there is a strong need for a non-destructive, water-tolerant method that can dynamically capture the biochemical changes responsible for soybean softening. Raman spectroscopy satisfies these requirements due to its insensitivity to water, specificity to molecular vibrations, and minimal sample preparation needs (Abreu et al., 2019; Almeida et al., 2011; Massei et al., 2024). Unlike other techniques, it allows direct detection of molecular transformations in cooking water without interference, offering flexible time-point insights into protein denaturation and pectin solubilization. Raman spectroscopy provides time-resolved monitoring of softening behavior during thermal processing, and advanced systems have been developed to function reliably even under high pressure and temperature in sealed environments.

The objectives of the study were to (1) investigate the molecular changes in proteins and pectin-derived acidic polysaccharides released into cooking water during soybean thermal processing using handheld Raman spectroscopy, (2) correlate spectral variations with chemical composition and texture measurements, and (3) develop a predictive model for the monitoring of softening progression over cooking time. This approach is expected to support improved control strategies in industrial processing environments and enhance product consistency.

2. Materials and methods

2.1. Soybean samples and sample preparation

Dried soybeans (Hokkaido Tokachi, Tokyo, Japan; initial moisture content 6.88 ± 0.18 % d.b.) were purchased from a local supermarket in Gifu, Japan and stored at room temperature (25 °C). The protein content was determined as 35.1 % by the Japan Food Research Laboratories (General Incorporated Association). Three soybeans (1.05 ± 0.02 g) were soaked in 6 mL of distilled water in a glass tube and incubated at 25 °C (MIR-154, PHC, Tokyo, Japan) for 24 h. The soaking procedure was adapted from previously reported methods (Agume et al., 2017) to promote water absorption and facilitate the softening process during boiling. After soaking, the tubes were subsequently boiled in a water bath at 90 °C for varying durations (0, 30, 60, 90, and 120 min), with the time intervals selected with reference to previous studies on bean softening under atmospheric pressure boiling (Anzaldúa-Morales et al., 1996). The sample of 0 min was used as the unheated control for comparison. For each sampling time moment, five replicate tubes were collected. The samples were rapidly cooled to 25 °C using an ice bath (for 30 s) to standardize the measurement conditions. Boiled water was analyzed using Raman spectroscopy and subjected to quantitative analysis of protein and pectin concentrations. Concurrently, the textural properties of the boiled soybeans, specifically hardness, were evaluated using instrumental texture analysis.

2.2. Hardness

The hardness, defined as the maximum force (N) of the samples, was measured via a penetration test using a texture analyzer (TA. XT Plus, Stable Micro Systems, Surrey, UK) equipped with a P/2 probe (2 mm) at 25 °C. The probe was inserted into the center position of the sample to 75 % strain at a penetration speed of 1 mm/s, following previously reported methods with slight modifications (Chigwedere et al., 2018; Taffire et al., 2024). Texture measurements were conducted on five replicate samples at each boiling time point.

2.3. Raman spectroscopy

Raman spectroscopy measurements were performed based on a previous study (Hirotsu et al., 2025). A PalmTop Raman Spectrometer (PR-1w, JASCO, Tokyo, Japan) was used with a measurement range of 3000–200 cm^{-1} . The maximum laser output was set to 50 mW with an exposure time of 1 s and 64 accumulations per measurement.

Samples of boiled water were taken at five different times during heating at the specified time points and analyzed using Raman spectroscopy. Two types of sample preparation methods were employed depending on whether an internal standard was used. The use of internal standards in Raman spectroscopy has been shown to correct variations in laser intensity and inner filter effects, thereby enhancing the reproducibility and accuracy of measurements (Diz et al., 2022). In this study, 50 % ethanol as an internal standard was added because of its stable Raman signal and minimal spectral interference with the target analytes in cooking water. These approaches aimed to ensure measurement consistency and accurate quantitative comparisons. For measurements without an internal standard, 10 μL of boiled solution was directly placed onto the dedicated sample container (JASCO measurement plate) of the Raman spectrometer. For measurements with internal standards, boiled solutions (8 μL) from each boiling time point were mixed with 50 % ethanol (2 μL). A distinct and consistent ethanol peak corresponding to C–C–O deformation vibration was observed at 1050 cm^{-1} (Zhang et al., 2025) and was used as a reliable internal reference for spectral normalization in this study. This peak did not interfere with the detection of protein- and pectin-related signals, thus supporting the suitability of ethanol as an internal standard for the Raman-based monitoring of soybean cooking water. This consistency supports the suitability of ethanol as an internal standard for Raman-based molecular analysis of complex food matrices, such as boiled soybean water. The measurements were repeated five times for each condition.

For samples containing the internal standard, spectra were normalized according to the following:

$$\text{Normalized Intensity} = I_{\text{sample}} / I_{\text{ethanol}} \quad (1)$$

2.4. Principal component analysis (PCA) for spectral characteristic analysis

PCA was conducted on normalized Raman spectra obtained from two kinds of sample conditions, with and without internal standard. This was done using MetaboAnalyst 6.0 (Xia Lab, McGill University, Montreal, Canada) to identify clustering patterns among samples at different boiling times. Spectral data underwent rigorous filtering as follows: (1) exclusion of features with a relative standard deviation > 25 % to minimize noise and (2) removal of low-variance features (lowest 40 % by interquartile range) and low-intensity signals. This approach was adapted from a previously reported method with modifications (Shen et al., 2016). All data were subsequently mean-centered and scaled to the unit variance. The first principal component (PC1), which explained the largest proportion of variance, was primarily used for subsequent analyses owing to its association with cooking duration trends.

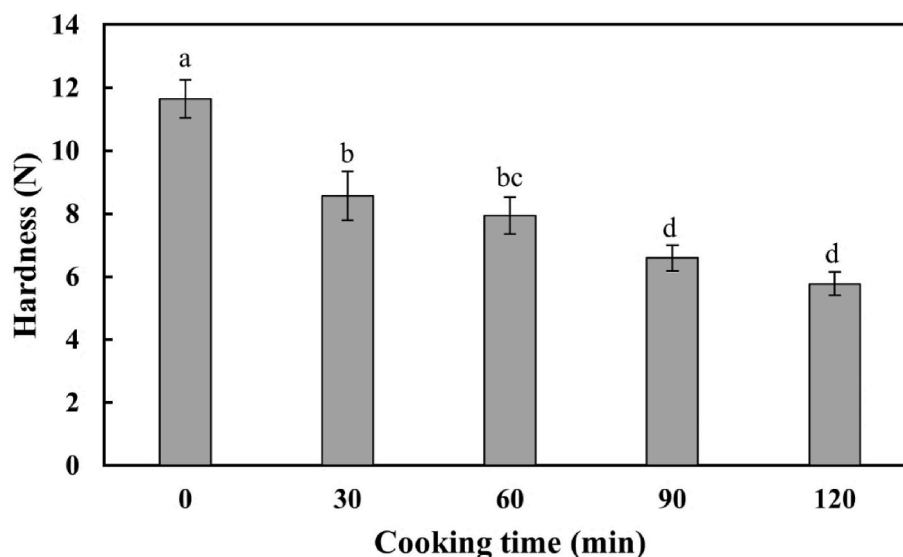


Fig. 1. Changes in soybean hardness during thermal processing at 90 °C over time. Error bars represent standard deviation (SD, n = 5). Different lowercase letters indicate statistically significant differences at $p < 0.05$ (Tukey–Kramer test).

The PCA loadings were calculated to identify the Raman shifts that contributed most significantly to the observed spectral variations. Critical Raman shifts were extracted from the PC1 loading plot, with absolute loading values greater than 0.7 considered significant, thereby indicating dominant contributions to spectral variation. This threshold was adopted based on criteria commonly used in PCA interpretation (Jolliffe, 2002). Peaks meeting this threshold were mapped to characteristic molecular vibrations for structural analysis during thermal processing.

2.5. Quantitative chemical analysis

2.5.1. Protein concentration

The protein concentration was determined based on Miranda (2024) via the Bradford method using a Bio-Rad Protein Assay Kit II (1.73 mg/mL, #5000002, Hercules, CA, USA). Bovine serum albumin (BSA) was used as the standard protein. The dye reagent was prepared by diluting one part of the Dye Reagent Concentrate with four parts of deionized water and filtering it through Whatman #1 filter paper to remove particulates. A standard curve was constructed using the following four concentrations of BSA: 0.05, 0.12, 0.38, and 0.5 mg/mL.

Samples of boiled water were collected at the predefined sampling time points and pre-diluted 10 times with distilled water before measurement. Each standard (10 μ L) and sample solution (10 μ L) were pipetted into separate wells of a microtiter plate, followed by the addition of 200 μ L of diluted dye reagent to each well. The sample and reagent mixture were thoroughly mixed using a microplate reader (Thermo Scientific™ Varioskan™ LUX, Waltham, MA, USA). The plate was incubated at 25 °C for 20 min to allow complete color development. Absorbance was measured at 595 nm using a microplate reader. All measurements were performed in triplicate, and the average values were used for data analysis.

2.5.2. Pectin concentration

The pectin concentration was measured based on Umehara et al. (2025) using the carbazole sulfate method. A mixture was prepared by combining 500 μ L of sulfuric acid (98 %) and 100 μ L of sample solution, which had been pre-diluted 50 times. After mixing, 20 μ L of carbazole reagent was added to the solution. The mixture was then heated at 100 °C for 20 min. Standard solutions of galacturonic acid (GalA) were prepared at concentrations of 0, 10, 20, 40, 80, and 160 μ g/mL. The absorbance was measured at 540 nm using a microplate reader.

2.6. SDS-PAGE electrophoresis

After centrifugation of each sample at 3000 \times g for 8 min, the supernatant was collected and heated at 95 °C for 5 min, then cooled to room temperature before loading.

Sodium dodecyl sulfate polyacrylamide gel electrophoresis (SDS-PAGE) was performed with a 12 % precast gel (Mini-PROTEAN TGX, Bio-Rad, USA) in a Bio-Rad mini-gel slab electrophoresis system (Bio-Rad Laboratories, Richmond, CA, USA). The volume of the protein marker (Spectra Multicolor Broad Range Protein Ladder, Thermo Scientific, USA) loaded was 5 μ L, and the volume of each sample was 20 μ L, respectively. Electrophoresis was conducted at a constant voltage of 200 V for 40 min, followed by staining with Bio-Safe Coomassie Stain (#1610786, Bio-Rad, USA).

2.7. Development of texture prediction model from Raman characteristics

The following four key Raman shifts were identified as substantial molecular markers: disulfide (S–S) bonds at 558 cm^{-1} , C–S bond at 682 cm^{-1} , glycosidic at 936 cm^{-1} (C–C stretching in polysaccharide backbone), 944 cm^{-1} (glycosidic bonds in pectin structures), and C–H deformation vibration at 1458 cm^{-1} . These spectral markers represent the molecular transformations occurring during boiling, which are closely associated with soybean softening behavior, as revealed by the chemical and textural measures in this study.

2.8. Statistical analysis

Statistical significance was determined for hardness, Raman intensity, the quantified solubilized components and correlation analyses of the samples under different cooking conditions. PCA was performed using MetaboAnalyst 6.0 to extract key features and identify clustering patterns in the Raman spectral data. Multiple comparisons between different cooking times points were conducted using the Tukey–Kramer test ($R \times 64$ 3.6.2, R Development Core Team, New Zealand), and p -value of less than 0.05 was considered statistically significant.

3. Results and discussion

3.1. Changes in soybean hardness during cooking

As shown in Fig. 1, soybean hardness decreased from 11.65 N at 0

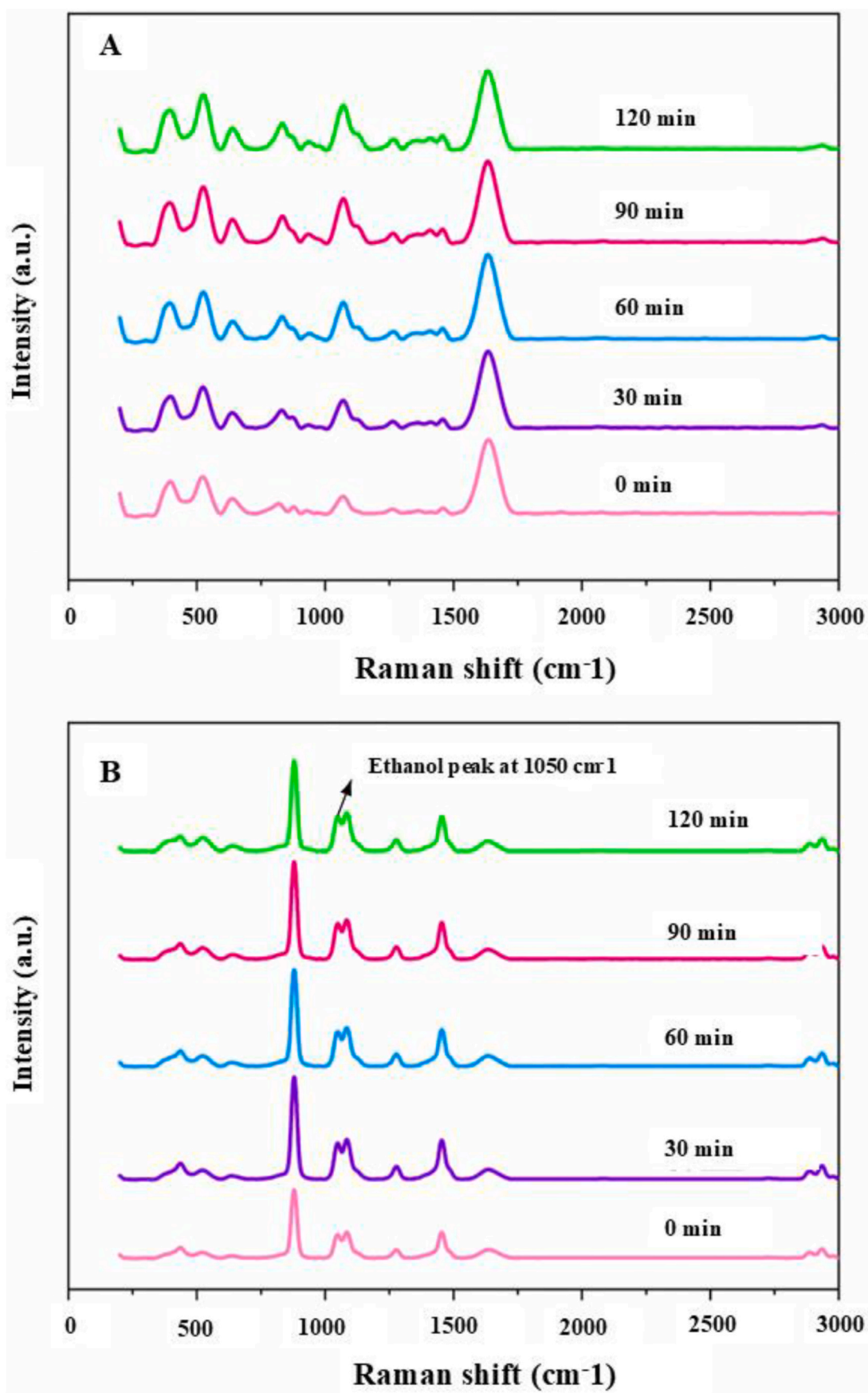


Fig. 2. Raw Raman spectral profiles of cooking water at different boiling times: (A) without internal standard and (B) with 50 % ethanol internal standard. The differences are due to intensity variation, not peak shifts or compositional changes, indicating improved reproducibility with ethanol normalization.

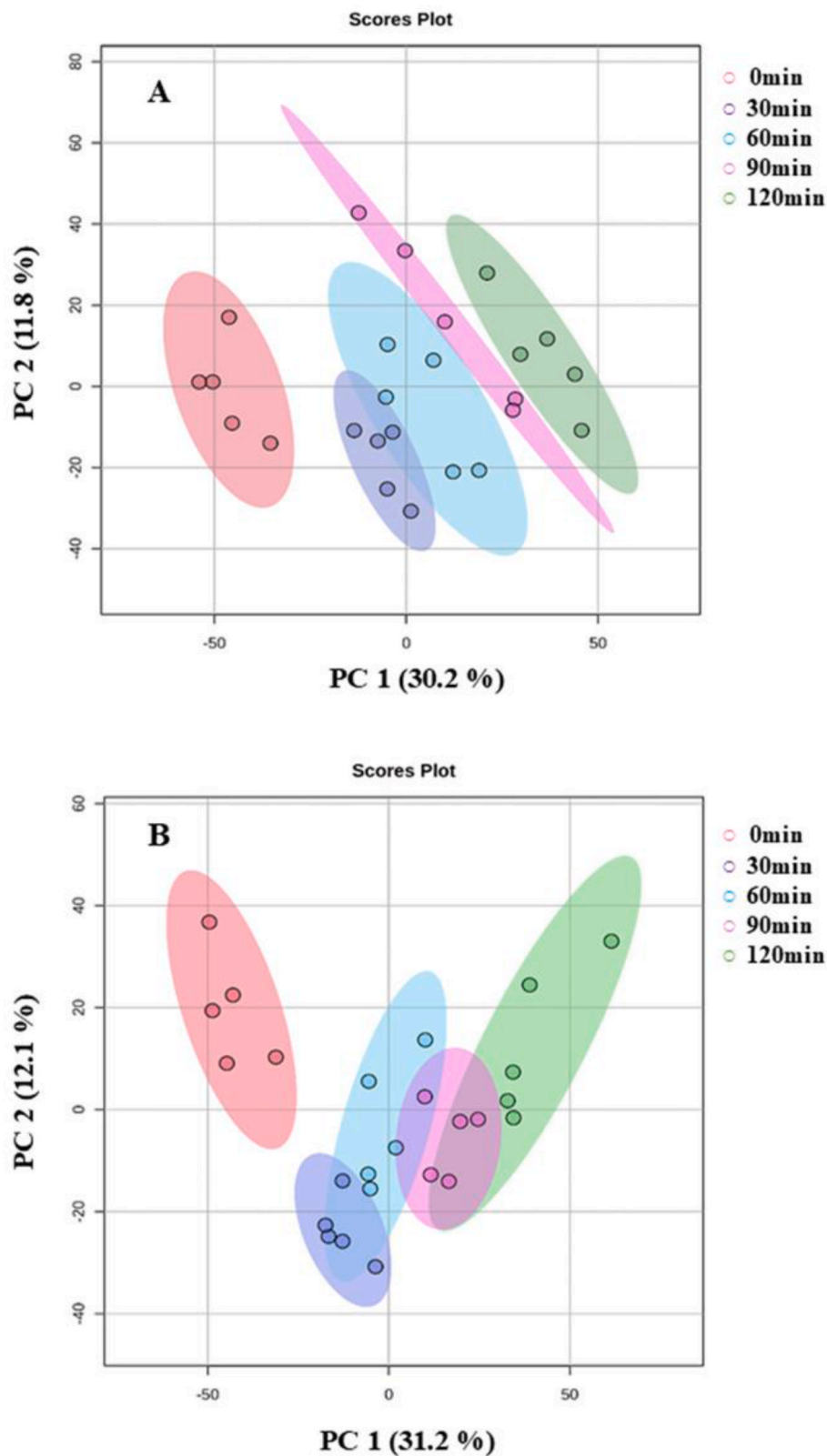


Fig. 3. PCA score plots of Raman spectra from cooking water at different boiling times: (A) without internal standard and (B) with 50 % ethanol internal standard.

min to 5.77 N at 120 min, indicating progressive softening, likely reflecting the breakdown of cellular integrity relevant to cooking texture. A statistically significant decrease in hardness was observed within the first 30 min ($p < 0.05$), indicating that softening initiates early in the cooking process. The decline in hardness further intensified

from 60 min onward, after which the value stabilized between 90 and 120 min.

This early reduction in hardness indicates the onset of structural breakdown, primarily due to the solubilization of pectic substances in the middle lamella, which weakens intercellular adhesion and initiates

Table 1

Comparison of Raman peak positions and intensities in cooking water samples with and without 50 % ethanol internal standard.

With 50 % ethanol		Without 50 % ethanol	
Raman shift (cm ⁻¹)	Absolute Loading Value	Raman shift (cm ⁻¹)	Absolute Loading Value
682	0.960	1087	0.996
558	0.951	631	0.990
936	0.944	534	0.983
491	0.931	824	0.979
640	0.925	403	0.960
377	0.912	932	0.925
519	0.912	1261	0.850
235	0.805	2937	0.763
298	0.801	690	0.737
964	0.759	856	0.734
1062	0.749	1156	0.732
919	0.745	585	0.730
335	0.725	906	0.715
695	0.715	338	0.705
464	0.713	1283	0.703
610	0.705	1241	0.701
410	0.704	1021	0.701
586	0.702	440	0.700

tissue disintegration (An et al., 2024). As heating continues, protein denaturation and continued pectin dissolution further compromise the structural integrity, accelerating softening. This interpretation is supported by previous studies reporting strong correlations between the solubilization of pectin or proteins and texture degradation. An et al. (2025) reported a strong negative correlation between pectin solubilization and bean hardness ($r = -0.977$; $p < 0.0001$), which supports the current finding of early and progressive softening linked to macromolecular changes. Similarly, protein denaturation has been shown to correlate with texture loss ($r = 0.96-0.99$), emphasizing its role in matrix destabilization during heating (Zhu, Che, et al., 2023). The combined dissolution of pectin and structural proteins, as demonstrated by Zahir et al. (2021), contributes to the weakening of intercellular adhesion and the disintegration of cellular structure, which helps explain the decline in hardness and tissue disintegration observed at later stages. Such findings enhance the connection observed in this study between texture degradation and the dissolution of structural macromolecules, including pectin and protein (Siqueira et al., 2013). The leaching of pectin and protein during softening offers a measurable signal that can be monitored by Raman spectroscopy to predict textural changes in cooked soybeans.

3.2. Raman spectral profile of soybean cooking water

3.2.1. Comparison of samples with and without internal standard

The Raman spectra of soybean cooking water at different boiling time points are presented in Fig. 2. The spectra were analyzed under the following two different conditions: without an internal standard (Fig. 2A) and with an internal standard (Fig. 2B). Progressive changes in spectral intensity were observed with increasing boiling time, without alteration of peak positions, indicating enhanced signal strength rather than changes in chemical composition. In Fig. 2A, although the overall spectra remain consistent, numerous small fluctuating peaks are observed, thereby resembling spectral noise. These fluctuations suggest variability in signal acquisition and limited reproducibility. By contrast, Fig. 2B shows sharper and more consistent peak profiles. This enhancement is attributed to the addition of ethanol as an internal standard. The stable peak at approximately 1050 cm⁻¹ provided a fixed reference for spectral normalization, thus effectively minimizing instrumental and sampling variability across measurements and ultimately improving the reliability and clarity of the spectra. Importantly, the ethanol peak of 1050 cm⁻¹ does not overlap with the key molecular regions used to analyze soybean-derived compounds, such as proteins

and pectin. This study follows widely accepted principles in spectral analysis, which suggest choosing reference peaks that do not mix with the main signals of target compounds (Aarnoutse & Westerhuis, 2005). These findings support the reliability of using a non-interfering internal standard in Raman spectroscopy to improve data reproducibility and interpretability during thermal processing, besides emphasize its capability for time-course monitoring or observation of compositional shifts within complex food matrices.

3.2.2. Identification of characteristic Raman bands

Improved spectral clarity enabled the consistent identification of major Raman bands related to the solubilized components. PCA, as shown in Fig. 3, revealed a time-dependent spectral variance across the boiling durations, particularly along PC1, which accounted for the largest proportion of the explained variation. Based on the PC1 loadings, specific Raman bands with absolute loading values greater than 0.7 were identified as the most influential contributors to this variance and are summarized in Table 1. These peaks include bands at 682 cm⁻¹ and 558 cm⁻¹, attributed to C-S bonds (methionine, cysteine) (Herrero, 2008; Li-Chan, 1996) and disulfide bonds in proteins (Lancelot et al., 2021) respectively. The peak at 936 cm⁻¹ is associated with the twisting vibration of the H-C (1)-C (5)-C (4) segment in glycosidic linkages of pectin (Xu et al., 2024). These vibrational modes are sensitive to changes in the protein conformation and pectin structure, and their high loading values indicate their dominant role in distinguishing samples at different boiling stages.

As shown in Fig. 3B, PCA revealed clearer intragroup clustering under standardized conditions, indicating improved spectral repeatability. Although the separation between boiling durations remained moderate, the use of an internal standard enhanced signal consistency, supporting the reliability of these measurements. PCA serves mainly as a qualitative visualization tool, and the observed group overlap may reflect the internal similarity in sample composition (Huang et al., 2018). Without internal standard, peaks at 1087, 631, and 534 cm⁻¹ showed greater variability, likely due to instrumental drift and sample concentration differences. Normalizing spectra to the ethanol peak at 1050 cm⁻¹ effectively compensated for these variations, adjusting signal intensities and improving reproducibility across measurements. These improvements in spectral consistency are consistent with previous findings emphasizing the importance of signal normalization for reliable quantitative analysis (Sebben et al., 2018; Silveira et al., 2009).

In addition to the major peaks identified through PCA, several weaker protein-related bands, such as Amide III (1240 cm⁻¹), C-H deformation (1458 cm⁻¹), and Amide I (1638 cm⁻¹), were also included in the subsequent correlation analysis. Although their intensities were relatively low, these bands are biochemically relevant markers of protein conformation (Meng et al., 2003; Rygula et al., 2013), hence, they were retained to explore their potential associations with the texture and chemical data.

3.3. Temporal trends in key Raman markers during boiling

3.3.1. Protein-related Raman band changes

Raman spectroscopy was used to analyze the leaching of protein-related molecular species into the cooking water over time. Fig. 4A-E shows the changes in intensity of the characteristic protein-associated Raman peaks over time. In Fig. 4A, the intensity of the peak at 558 cm⁻¹, attributed to disulfide (S-S) bonds, increased significantly with boiling time ($p < 0.05$), thereby suggesting progressive release of disulfide-containing protein fragments into the water. This may be linked to thermal unfolding and solubilization of denatured proteins. Interestingly, Berhe et al. (2014) reported a decline in the S-S stretching intensity in meat samples due to thermal cleavage; however, in this study an increase was observed in cooking water. Similar trends have also been reported in heated soy protein isolates, where structural changes involving disulfide bond cleavage and migration were

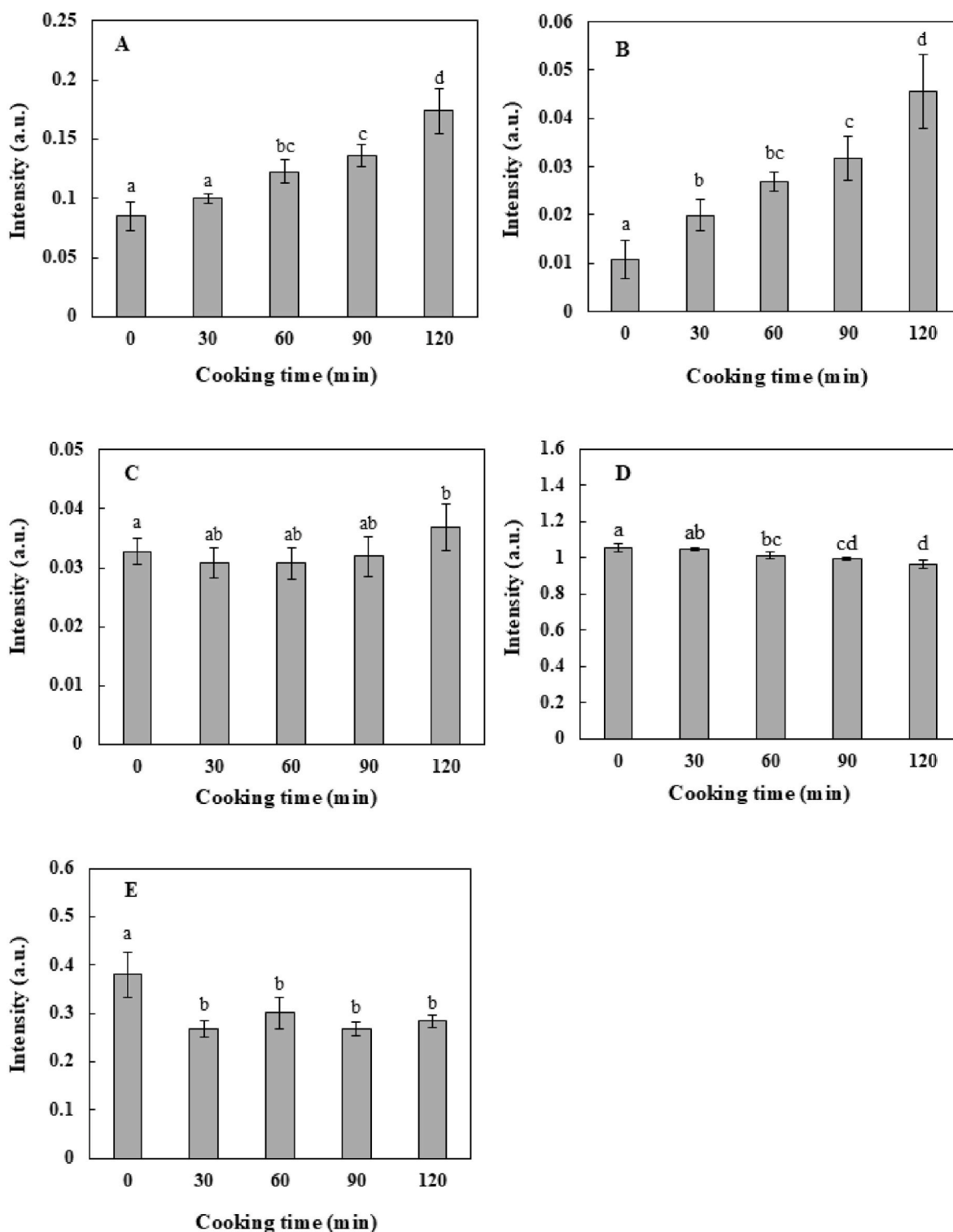


Fig. 4. Changes in Raman intensities of protein-related bands during boiling. (A) Disulfide (S-S) bonds at 558 cm^{-1} ; (B) C-S bonds at 682 cm^{-1} ; (C) Amide III at 1240 cm^{-1} ; (D) C-H deformation at 1458 cm^{-1} ; (E) Amide I at 1638 cm^{-1} . Error bars represent standard deviation (SD, $n = 5$). Different lowercase letters indicate statistically significant differences at $p < 0.05$ (Tukey-Kramer test).

identified by Raman spectroscopy (Herrero et al., 2009; Yin et al., 2019). Such findings support the notion that boiling promotes the release of soluble disulfide-containing fragments into the aqueous phase. This discrepancy likely reflects the migration and accumulation of cleaved disulfide-containing fragments into the aqueous phase rather than their presence in the tissue itself. This suggests that bond rupture promotes migration into the aqueous phase, which explains the observed upward

trend. Similarly, the C-S bond peak at 682 cm^{-1} in Fig. 4B, which is commonly associated with methionine or cysteinyl residues, showed a notable upward trend, thus indicating increased presence of these sulfur-containing amino acid fragments in the soluble phase. A comparable increase in Raman intensity due to the exposure or oxidation of sulfur-based groups has also been reported under different protein disruption conditions, such as freezing-induced peptide cleavage (Yan

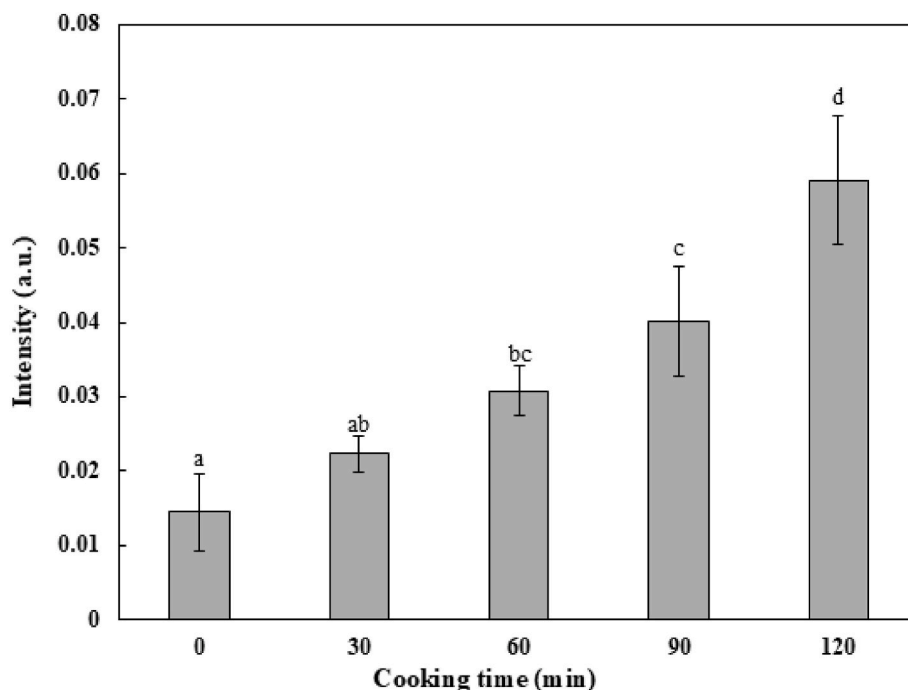


Fig. 5. Changes in Raman intensity of the glycosidic linkage band at 936 cm^{-1} during boiling. Error bars represent standard deviation (SD, $n = 5$). Different lowercase letters indicate statistically significant differences at $p < 0.05$ (Tukey–Kramer test).

et al., 2020). This further supports the sensitivity of this band to structural changes involving sulfur-rich residues. The Amide III band at 1240 cm^{-1} (Fig. 4C), which reflects peptide backbone vibrations, moderately increased over time. This observation is consistent with previous findings that attribute Amide III changes to peptide bond cleavage and conformational alterations during heating (Mikhonin et al., 2004). Conversely, the C–H deformation peak at 1458 cm^{-1} (Fig. 4D), which is typically linked to aliphatic side chains, gradually decreased. This may reflect the degradation or loss of solubility of hydrophobic moieties during extended heating. Moreover, the Amide I peak at 1638 cm^{-1} (Fig. 4E), which is associated with C=O stretching in peptide bonds, also declined. This may indicate aggregation or loss of solubility of higher molecular weight protein fragments (Wang et al., 2024). These combined trends suggest that prolonged heating leads to the partial breakdown and diffusion of specific protein structures, with characteristic Raman signals reflecting their time-dependent transformation and release behavior.

3.3.2. Glycosidic band changes reflecting pectin solubilization

In addition to protein-related changes, the Raman band at 936 cm^{-1} (Fig. 5), which is attributed to glycosidic linkages or C–C stretching within the sugar backbone of pectic substances, displayed a continuous increase throughout the boiling period. The steady increase in intensity suggested the progressive release of pectin and related polysaccharides, including hemicellulose, into the aqueous phase. This trend is consistent with the thermal softening of plant cell walls, in which heat disrupts the middle lamella and releases GalA-rich polysaccharides. As pectin dissolves, glycosidic vibrations become increasingly detectable in the Raman spectra (Pu et al., 2024; Wiercigroch et al., 2017). The study results reinforce the utility of the 936 cm^{-1} band as a molecular marker for tracking the leaching of carbohydrate structures during thermal treatment. Combined with the observed protein-related spectral changes, the behavior of this peak contributes to a comprehensive understanding of the responses of the soybean structural components to boiling.

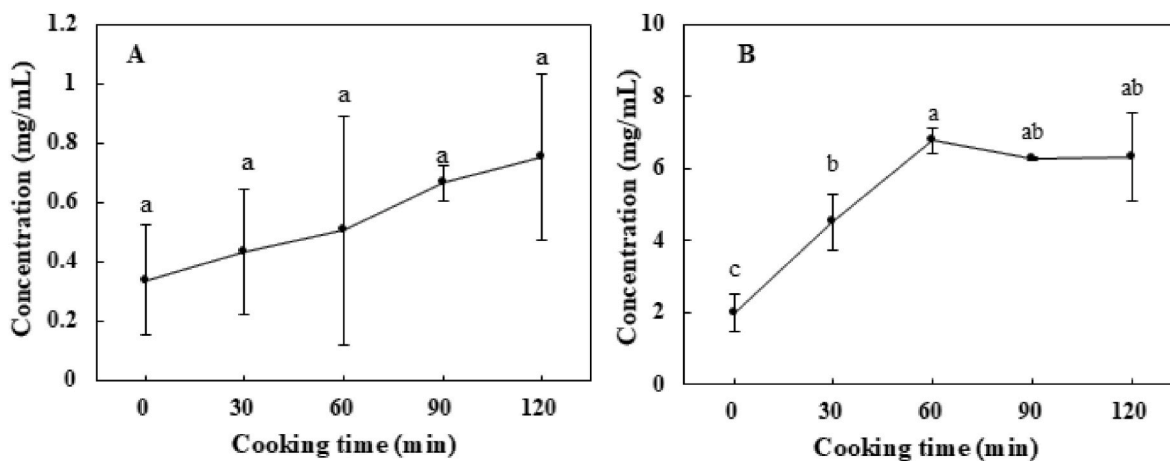


Fig. 6. Quantification of solubilized components in cooking water at different boiling times: (A) protein concentration (mg/mL), (B) pectin concentration (mg/mL). Error bars represent standard deviation (SD, $n = 5$). Different lowercase letters indicate statistically significant differences at $p < 0.05$ (Tukey–Kramer test).

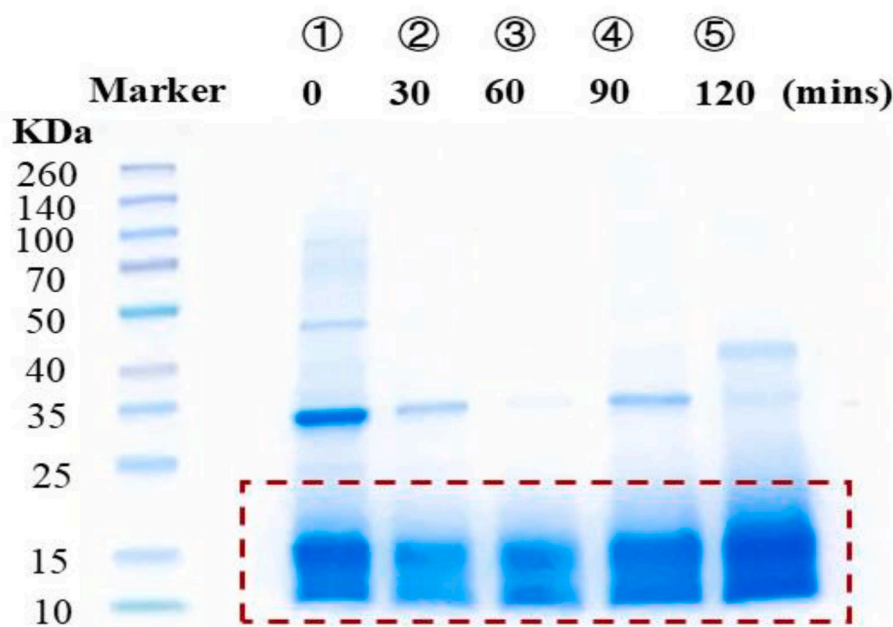


Fig. 7. SDS-PAGE of proteins released into the cooking water. Lanes 1–5, 0/30/60/90/120 min respectively. Red boxed region indicates the LMW smear (~10–25 kDa).

3.4. Solubilization of protein and pectin components

Protein concentration in the cooking water increased from 0.34 ± 0.18 mg/mL at 0 min to 0.75 ± 0.28 mg/mL at 120 min (Fig. 6A). However, the differences between time points were not statistically significant. Based on the measured seed protein content 35.1 % for this study, the soluble protein concentration remained below 1 mg/mL at 120 min, indicating limited apparent solubilization. This interpretation was consistent with the SDS-PAGE results (Fig. 7), which showed a persistent low molecular weight smear (10–25 kDa range, marked by red boxed region) across time and no gel-top accumulation. At 0 min, a 35–45 kDa band was also observed, which was attributed to diffusion during the pre-heating soaking step. This band corresponds to the acidic subunits of glycinin (Cho et al., 2025) and disappeared after 30 min of heating. Although quantitative analysis indicated that the concentration of solubilized protein remained low, Raman spectroscopy sensitively reflected even limited solubilization as intensity differences, particularly due to the strong responses of S–S and C–S vibrations.

Pectin concentration rose rapidly from 1.99 ± 0.52 mg/mL to 6.32 ± 1.21 mg/mL within the first 60 min (Fig. 6B) and then plateaued. This behavior suggested an early breakdown of the middle lamella and cell walls, followed by a saturation point at which the most extractable pectin was released. Statistically significant differences ($p < 0.05$) were observed between the samples at different boiling time points, thus supporting the progressive and time-dependent solubilization of pectin (Kyomugasho et al., 2023).

3.5. Prediction of soybean hardness based on Raman spectral changes

Regression analysis (Fig. 8A and B) revealed strong negative correlations between soybean hardness and Raman bands corresponding to disulfide bonds (558 cm^{-1} , $R^2 = 0.69$) and C–S bonds (682 cm^{-1} , $R^2 = 0.73$). These results suggest that sulfur-containing protein fragments accumulate in water due to thermal denaturation and solubilization, thereby contributing to soybean softening. Additionally, C–H deformation at 1458 cm^{-1} showed a moderate positive correlation ($R^2 = 0.57$, Fig. 8C), which may reflect retention of certain hydrophobic moieties in harder samples. Overall, these trends demonstrated that the Raman

signatures of protein breakdown were closely linked to texture degradation.

The 936-cm^{-1} peak, which is associated with glycosidic linkages in pectin and related polysaccharides, showed a strong negative correlation with hardness ($R^2 = 0.70$, Fig. 8D). This indicates that increased solubilization of the pectin structures corresponds to decreased hardness. As cell wall polysaccharides dissolve and the middle lamellar integrity diminishes, soybean tissues lose their structural rigidity. These findings confirm that Raman detection of carbohydrate solubilization, particularly via the 936-cm^{-1} peak, serves as an effective molecular indicator of thermal softening.

Raman spectral features reflecting both protein and pectin solubilization were reliable predictors of soybean textural changes. This reinforces the utility of this nondestructive technique in time-dependent food quality monitoring applications.

4. Conclusion

This study establishes the utility of Raman spectroscopy as a reliable tool for capturing molecular changes in boiled soybean water during thermal processing. The changes in intensity over time of specific Raman bands, especially those related to protein denaturation and pectin solubilization, corresponded with the quantified concentrations of solubilized components. Meanwhile, a progressive decline in soybean hardness was observed, reflecting cumulative cell wall degradation and matrix softening.

The clear correlation between these molecules and soybean softening was further supported by the strong relationship between the C–S bond (682 cm^{-1}), glycosidic linkage band (936 cm^{-1}) and texture loss, emphasizing their potential as non-destructive indicators of structural breakdown. SDS-PAGE and protein quantification indicated limited protein leaching, whereas Raman spectroscopy remained sensitive to protein-related signals, reflecting the strong response of S–S and C–S vibrations even at low solubilization amounts.

In summary, the results support a direct link between solubilization processes and softening behavior, showing that Raman spectral markers can be used to monitor texture in flexible time. This non-destructive approach is suitable for integration into industrial cooking systems,

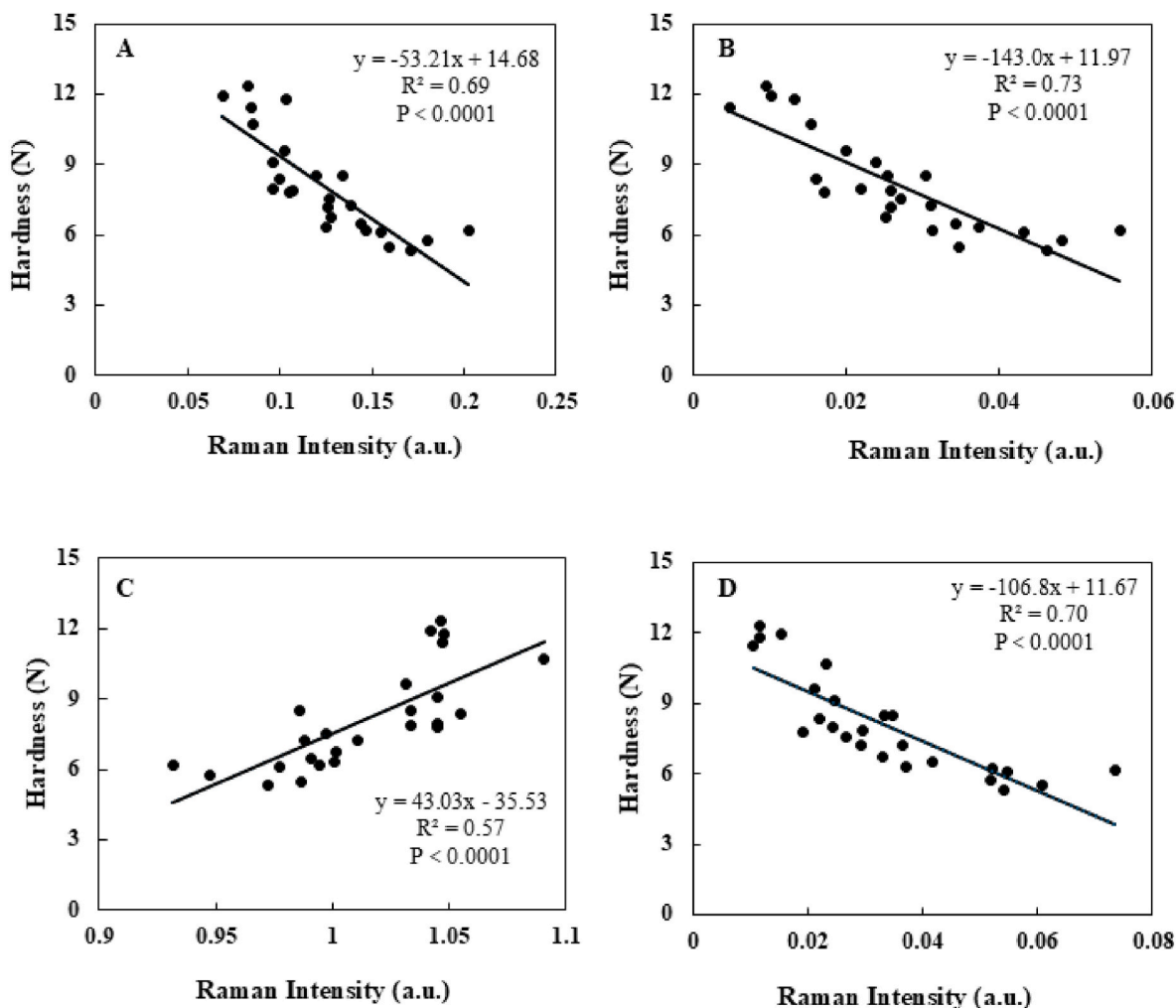


Fig. 8. Correlation analysis between Raman band intensities and soybean hardness: (A) disulfide (S-S) bonds at 558 cm⁻¹; (B) C-S bonds at 682 cm⁻¹; (C) C-H deformation at 1458 cm⁻¹; (D) glycosidic linkages at 936 cm⁻¹.

enabling improved process control and product uniformity. Furthermore, the findings offer a foundation for extending Raman-based texture prediction to other legumes and diverse thermal environments, thus facilitating broader optimization across food processing systems.

CRediT authorship contribution statement

Wenchao Li: Writing – review & editing, Writing – original draft, Visualization, Validation, Software, Resources, Investigation, Formal analysis, Data curation. **Takashi Watanabe:** Writing – review & editing, Supervision. **Kasumi Nakagawa:** Data curation. **Takahisa Nishizu:** Writing – review & editing, Supervision. **Tepei Imaizumi:** Writing – review & editing, Validation, Supervision, Project administration, Methodology, Funding acquisition, Data curation, Conceptualization.

Declaration of competing interest

The authors declare the following financial interests/personal relationships which may be considered as potential competing interests: Tepei Imaizumi reports financial support was provided by Japan Society for the Promotion of Science. If there are other authors, they declare that they have no known competing financial interests or personal relationships that could have appeared to influence the work reported in this paper.

Acknowledgments

This research was supported by JSPS KAKENHI Grant Number 24K21263.

Appendix A. Supplementary data

Supplementary data to this article can be found online at <https://doi.org/10.1016/j.lwt.2025.118535>.

Data availability

Data will be made available on request.

References

- Aarnoutse, P. J., & Westerhuis, J. A. (2005). Quantitative Raman reaction monitoring using the solvent as internal standard. *Analytical Chemistry*, 77(5), 1228–1236. <https://doi.org/10.1021/ac0401523>
- Abreu, G. F., Borém, F. M., Oliveira, L. F. C., Almeida, M. R., & Alves, A. P. C. (2019). Raman spectroscopy: A new strategy for monitoring the quality of green coffee beans during storage. *Food Chemistry*, 287, 241–248. <https://doi.org/10.1016/j.foodchem.2019.02.019>
- Agume, A. S. N., Njintang, N. Y., & Mbofung, C. M. F. (2017). Effect of soaking and roasting on the physicochemical and pasting properties of soybean flour. *Foods*, 6(2), 12. <https://doi.org/10.3390/FOODS6020012>
- Almeida, M. R., Oliveira, K. D. S., Stephani, R., & De Oliveira, L. F. C. (2011). Fourier-transform Raman analysis of milk powder: A potential method for rapid quality

- screening. *Journal of Raman Spectroscopy*, 42(7), 1548–1552. <https://doi.org/10.1002/JRS.2893>
- An, N. T. H., Mathew, A., Tafiire, H., Van Loey, A., & Hendrickx, M. E. (2025). Behavior of common beans under two conditions of water accessibility during cooking: Essential role of pectin solubilization in bean softening. *Food Structure*, 44, Article 100416. <https://doi.org/10.1016/j.FOODSTR.2025.100416>
- An, N. T. H., Namutebi, P., Van Loey, A., & Hendrickx, M. E. (2024). Quantitative assessment of molecular, microstructural, and macroscopic changes of red kidney beans (*Phaseolus vulgaris* L.) during cooking provides detailed insights in their cooking behavior. *Food Research International*, 181, Article 114098. <https://doi.org/10.1016/j.FOODRES.2024.114098>
- Anzaldúa-Morales, A., Quintero, A., & Balandrán, R. (1996). Kinetics of thermal softening of six legumes during cooking. *Journal of Food Science*, 61(1), 167–170. <https://doi.org/10.1111/J.1365-2621.1996.TB14751.X>
- Aryee, A. N. A., Agyei, D., & Udenigwe, C. C. (2018). Impact of processing on the chemistry and functionality of food proteins. In R. Y. Yada (Ed.), *Proteins in food processing* (2nd ed., pp. 27–45). Woodhead Publishing. <https://doi.org/10.1016/B978-0-08-100722-8.00003-6>
- Berhe, D. T., Engelsens, S. B., Hviid, M. S., & Lametsch, R. (2014). Raman spectroscopic study of effect of the cooking temperature and time on meat proteins. *Food Research International*, 66, 123–131. <https://doi.org/10.1016/j.FOODRES.2014.09.010>
- Bizzani, M., William Menezes Flores, D., Alberto Colnago, L., & David Ferreira, M. (2020). Monitoring of soluble pectin content in orange juice by means of MIR and TD-NMR spectroscopy combined with machine learning. *Food Chemistry*, 332, Article 127383. <https://doi.org/10.1016/j.FOODCHEM.2020.127383>
- Chang, K., Shinzawa, H., & Chung, H. (2018). Concentration determination of inorganic acids that do not absorb near-infrared (NIR) radiation through recognizing perturbed NIR water bands by them and investigation of accuracy dependency on their acidities. *Microchemical Journal*, 139, 443–449. <https://doi.org/10.1016/j.MICROC.2018.03.019>
- Chen, R., Williams, P. A., Shu, J., Luo, S., Chen, J., & Liu, C. (2022). Pectin adsorption onto and penetration into starch granules and the effect on the gelatinization process and rheological properties. *Food Hydrocolloids*, 129, Article 107618. <https://doi.org/10.1016/j.FOODHYD.2022.107618>
- Chigwedere, C. M., Olaoye, T. F., Kyomugasho, C., Jamsazzadeh Kermani, Z., Pallares Pallares, A., Van Loey, A. M., Grauwet, T., & Hendrickx, M. E. (2018). Mechanistic insight into softening of Canadian wonder common beans (*Phaseolus vulgaris*) during cooking. *Food Research International*, 106, 522–531. <https://doi.org/10.1016/j.FOODRES.2018.01.016>
- Cho, E. S., Kim, S., Moon, J.-K., Park, S.-K., Maruyama, N., Wang, S., Lee, C.-H., & Lee, J.-Y. (2025). Identification and quantification of soybean 11S and 7S globulins using RP-UPLC. *Food Chemistry*, 473, Article 143019. <https://doi.org/10.1016/j.foodchem.2025.143019>
- Diz, E. L., Portela, R., Bañares, M. A., Charitidis, C., Ntziouni, A., Li, X., Thomson, J., & Xiarchos, I. (2022). Review of existing standards, guides, and practices for Raman spectroscopy. *Applied Spectroscopy*, 76, 747–772. <https://doi.org/10.1364/AS.76.000747>
- Herrero, A. M. (2008). Raman spectroscopy for monitoring protein structure in muscle food systems. *Critical Reviews in Food Science and Nutrition*, 48(6), 512–523. <https://doi.org/10.1080/10408390701537385>
- Herrero, A. M., Jiménez-Colmenero, F., & Carmona, P. (2009). Elucidation of structural changes in soy protein isolate upon heating by Raman spectroscopy. *International Journal of Food Science and Technology*, 44(4), 711–717. <https://doi.org/10.1111/j.1365-2621.2008.01880.x>
- Hirotsu, Y., Thomas, M. L., Takeoka, Y., Rikukawa, M., & Yoshizawa-Fujita, M. (2025). Effect of cation side-chain structure on the physicochemical properties of pyrrolidinium-based electrolytes upon mixing with sodium salt. *Science and Technology of Advanced Materials*, 26(1), Article 2466417. <https://doi.org/10.1080/14686996.2025.2466417>
- Huang, L., Zhang, X., & Zhang, Z. (2018). Sensor array for qualitative and quantitative analysis of metal ions and metal oxyanion based on colorimetric and chemometric methods. *Analytica Chimica Acta*, 1044, 119–130. <https://doi.org/10.1016/j.ACA.2018.07.052>
- Jolliffe, I. T. (2002). Principal component analysis and factor analysis. In *Principal component analysis* (2nd ed., pp. 150–166). Springer. <https://doi.org/10.1007/b98835>
- Kong, Y., Sun, L., Wu, Z., Li, Y., Kang, Z., Xie, F., & Yu, D. (2023). Effects of ultrasonic treatment on the structural, functional properties and beany flavor of soy protein isolate: Comparison with traditional thermal treatment. *Ultrasonics Sonochemistry*, 101, Article 106675. <https://doi.org/10.1016/j.ULTSONCH.2023.106675>
- Kyomugasho, C., Wainaina, I., Grauwet, T., Van Loey, A., & Hendrickx, M. E. (2023). Bean softening during hydrothermal processing is greatly limited by pectin solubilization rather than protein denaturation or starch gelatinization. *Food Research International*, 165, Article 112471. <https://doi.org/10.1016/j.FOODRES.2023.112471>
- Lancelot, E., Fontaine, J., Grua-Priol, J., Assaf, A., Thouand, G., & Le-Bail, A. (2021). Study of structural changes of gluten proteins during bread dough mixing by Raman spectroscopy. *Food Chemistry*, 358, Article 129916. <https://doi.org/10.1016/j.FOODCHEM.2021.129916>
- Li-Chan, E. C. Y. (1996). The applications of Raman spectroscopy in food science. *Trends in Food Science & Technology*, 7(11), 361–370. [https://doi.org/10.1016/S0924-2244\(96\)10037-6](https://doi.org/10.1016/S0924-2244(96)10037-6)
- Liu, Z., Parida, S., Prasad, R., Pandey, R., Sharma, D., & Barman, I. (2022). Vibrational spectroscopy for decoding cancer microbiota interactions: Current evidence and future perspective. *Seminars in Cancer Biology*, 86, 743–752. <https://doi.org/10.1016/j.SEMCANCER.2021.07.004>
- Lukacs, M., Somogyi, T., Mukite, B. M., Vitális, F., Kovacs, Z., Rédey, Á., Stefaniga, T., Zsom, T., Kiskó, G., & Zsom-Muha, V. (2025). Investigation of the ultrasonic treatment-assisted soaking process of different red kidney beans and compositional analysis of the soaking water by NIR spectroscopy. *Sensors*, 25, 313. <https://doi.org/10.3390/S25020313>
- Massei, A., Falco, N., & Fissore, D. (2024). Use of Raman spectroscopy and PCA for quality evaluation and out-of-specification identification in biopharmaceutical products. *European Journal of Pharmacology and Biopharmaceutics*, 200, Article 114342. <https://doi.org/10.1016/j.EJPB.2024.114342>
- Meng, G., Ma, C.-Y., & Phillips, D. L. (2003). Rapid communication Raman spectroscopic study of globulin from *Phaseolus angularis* (red bean). *Food Chemistry*, 81(3), 411–420. [https://doi.org/10.1016/S0308-8146\(02\)00471-5](https://doi.org/10.1016/S0308-8146(02)00471-5)
- Mikhonin, A. V., Ahmed, Z., Ianou, A., & Asher, S. A. (2004). Assignments and conformational dependencies of the amide III peptide backbone UV resonance Raman bands. *Journal of Physical Chemistry B*, 108(49), 19020–19028. <https://doi.org/10.1021/jp045959d>
- Miranda, M. P. (2024). Comparison of the effect of Sodium Chloride concentration on protein determination: Bradford and Biuret methods. *Analytical Biochemistry*, 687, Article 115450. <https://doi.org/10.1016/j.AB.2023.115450>
- Pedone, I. S., Narita, I. M. P., da Silveira, M. M., Bassinello, P. Z., Vanier, N. L., & Colussi, R. (2024). Enhancing quick-cooking bean quality: The impact of salt concentrations on soaking of fresh and aged Brazilian genotypes. *Food and Humanity*, 3, Article 100422. <https://doi.org/10.1016/j.FOOHUM.2024.100422>
- Pu, Y., Zhao, M., O'Donnell, C., & O'Shea, N. (2024). Investigation of near infrared and Raman fibre optic process sensors for protein determination in milk protein concentrate. *Food and Bioprocess Processing*, 148, 218–228. <https://doi.org/10.1016/j.fbp.2024.09.013>
- Rahman, M. M., Hossain, M. M., Anwar, M. P., & Juraimi, A. S. (2011). Plant density influence on yield and nutritional quality of soybean seed. *Asian Journal of Plant Sciences*, 10(2), 125–132. <https://doi.org/10.3923/AJPS.2011.125.132>
- Rygula, A., Majzner, K., Marzec, K. M., Kaczor, A., Pilarczyk, M., & Baranska, M. (2013). Raman spectroscopy of proteins: A review. *Journal of Raman Spectroscopy*, 44, 1061–1076. <https://doi.org/10.1002/jrs.4335>
- Sasipriya, G., & Siddhuraju, P. (2012). Effect of different processing methods on antioxidant activity of underutilized legumes, Entada scandens seed kernel and Canavalia gladiata seeds. *Food and Chemical Toxicology*, 50(8), 2864–2872. <https://doi.org/10.1016/j.FCT.2012.05.048>
- Sebben, J. A., da Silveira Espindola, J., Ranzan, L., Fernandes de Moura, N., Trierweiler, L. F., & Trierweiler, J. O. (2018). Development of a quantitative approach using Raman spectroscopy for carotenoids determination in processed sweet potato. *Food Chemistry*, 245, 1224–1231. <https://doi.org/10.1016/j.FOODCHEM.2017.11.086>
- Shen, X., Gong, X., Cai, Y., Guo, Y., Tu, J., Li, H., Zhang, T., Wang, J., Xue, F., & Zhu, Z.-J. (2016). Normalization and integration of large-scale metabolomics data using support vector regression. *Metabolomics*, 12, 89. <https://doi.org/10.1007/s11306-016-1026-5>
- Silveira, L., Moreira, L. M., Conceição, V. G. B., Casalechi, H. L., Muñoz, I. S., Da Silva, F. F., Silva, M. A. S. R., De Souza, R. A., & Pacheco, M. T. T. (2009). Determination of sucrose concentration in lemon-type soft drinks by dispersive Raman spectroscopy. *Spectroscopy*, 23(3–4), 217–226. <https://doi.org/10.3233/SPE-2009-0383>
- Siqueira, B., dos, S., Vianello, R. P., Fernandes, K. F., & Bassinello, P. Z. (2013). Hardness of carioca beans (*Phaseolus vulgaris* L.) as affected by cooking methods. *LWT*, 54(1), 13–17. <https://doi.org/10.1016/j.LWT.2013.05.019>
- Tafiire, H., Wainaina, I. N., Lugumira, R., An, N. T. H., Ogwok, P., Grauwet, T., & Hendrickx, M. E. (2024). A detailed study on the cooking kinetics of fresh and hard to cook common beans (*Phaseolus vulgaris* L.): A case study on bean accessions of different market classes. *Journal of Food Engineering*, 381, Article 112186. <https://doi.org/10.1016/j.JFOODENG.2024.112186>
- Umehara, A., Oshima, T., Deshmukh, O. S., Nishizu, T., & Imaizumi, T. (2025). Detection of cell membrane disruption using electrical impedance spectroscopy and acceleration of cell wall modification in carrot processed under low temperature blanching. *Journal of Food Engineering*, 385, Article 112270. <https://doi.org/10.1016/j.JFOODENG.2024.112270>
- Van Buren, J. P. (1979). The chemistry of texture in fruits and vegetables. *Journal of Texture Studies*, 10(1), 1–23. <https://doi.org/10.1111/J.1745-4603.1979.TB01305.X>
- Wang, Y., Zhang, C., Yu, R., Wu, Z., Wang, Y., Wang, W., & Lai, Y. (2024). Robust and sensitive determination of nitrites in pickled food by surface-enhanced Raman spectroscopy. *Spectrochimica Acta Part A: Molecular and Biomolecular Spectroscopy*, 309, Article 123794. <https://doi.org/10.1016/j.SAA.2023.123794>
- Wiercigroch, E., Szafraniec, E., Czamara, K., Pacia, M. Z., Majzner, K., Kochan, K., Kaczor, A., Baranska, M., & Malek, K. (2017). Raman and infrared spectroscopy of carbohydrates: A review. *Spectrochimica Acta - Part A: Molecular and Biomolecular Spectroscopy*, 185, 317–335. <https://doi.org/10.1016/j.saa.2017.05.045>
- Xu, M. L., Gao, Y., & Han, X. X. (2024). Structure information analysis and relative content determination of protein and chitin from yellow mealworm larvae using Raman spectroscopy. *International Journal of Biological Macromolecules*, 272, Article 132787. <https://doi.org/10.1016/j.ijbiomac.2024.132787>
- Yan, B., Jiao, X., Zhu, H., Wang, Q., Huang, J., Zhao, J., Cao, H., Zhou, W., Zhang, W., Ye, W., Zhang, H., & Fan, D. (2020). Chemical interactions involved in microwave heat-induced surimi gel fortified with fish oil and its formation mechanism. *Food Hydrocolloids*, 105, Article 105779. <https://doi.org/10.1016/j.FOODHYD.2020.105779>
- Yin, H., Huang, J., & Zhang, H. (2019). Study on isolation and Raman spectroscopy of glycinin in soybean protein. *Grain & Oil Science and Technology*, 1(2), 72–76. <https://doi.org/10.3724/sp.j.1447.gost.2018.18002>

- Zahir, M., Fogliano, V., & Capuano, E. (2021). Soybean germination limits the role of cell wall integrity in controlling protein physicochemical changes during cooking and improves protein digestibility. *Food Research International*, 143. <https://doi.org/10.1016/j.foodres.2021.110254>
- Zhang, L., & McCarthy, M. J. (2013). NMR study of hydration of navy bean during cooking. *LWT*, 53(2), 402–408. <https://doi.org/10.1016/J.LWT.2013.03.011>
- Zhang, J., Qu, G., Lu, X., Ma, J., Wu, G., & Tan, Y. (2025). Insights on hydrophobic groups and Raman characteristics in an ethanol-water system. *Journal of Molecular Structure*, 1334, Article 141843. <https://doi.org/10.1016/J.MOLSTRUC.2025.141843>
- Zhu, L., Che, A. J. C., Kyomugasho, C., Chen, D., & Hendrickx, M. (2023). Effect of biochemical changes due to conventional ageing or chemical soaking on the texture changes of common beans during cooking. *Food Research International*, 173, Article 113377. <https://doi.org/10.1016/J.FOODRES.2023.113377>
- Zhu, L., Seufert, J., Kyomugasho, C., Chen, D., & Hendrickx, M. (2023). Mechanistic understanding of the effect of sodium citrate soaking of red kidney beans on their cooking behaviour. *LWT*, 187, Article 115303. <https://doi.org/10.1016/J.LWT.2023.115303>